Journal of Computational Physics 228 (2009) 123–136

Contents lists available at ScienceDirect

Journal of Computational Physics

journal homepage: www.elsevier.com/locate/jcp

A meshless method for solving an inverse spacewise-dependent heat source problem

Liang Yan, Feng-Lian Yang, Chu-Li Fu *

School of Mathematics and Statistics, Lanzhou University, Lanzhou 730000, China

ARTICLE INFO

Article history:
Received 20 March 2008
Received in revised form 19 August 2008
Accepted 2 September 2008
Available online 8 September 2008

Keywords:
Meshless method
Method of fundamental solutions
Heat source
Ill-posed problem

ABSTRACT

In this paper an effective meshless and integration-free numerical scheme for solving an inverse spacewise-dependent heat source problem is proposed. Due to the use of the fundamental solution as basis functions, the method leads to a global approximation scheme in both spatial and time domains. The standard Tikhonov regularization technique with the generalized cross-validation criterion for choosing the regularization parameter is adopted for solving the resulting ill-conditioned system of linear algebraic equations. The effectiveness of the algorithm is illustrated by several numerical examples.

1. Introduction

In the process of transportation, diffusion and conduction of natural materials, the following heat equation is a suitable approximation:

$$u_t - \Delta u = f(x,t;u), \quad (x,t) \in \Omega \times (0, t_{\max}), \tag{1.1}$$

where u represents the state variable, Ω is a bounded domain in R^d, and the right hand side f denotes physical laws, in our case source terms. Unfortunately, the characteristics of sources in actual problems are always unknown. These are inverse problems, and it is well-known that they are generally ill-posed, i.e. the existence, uniqueness and stability of their solutions are not always guaranteed [1]. In general, a complete recovery of the unknown source is not attainable from practically restricted boundary measurements. If no *a priori* information is available on the functional form of the unknown variable, the solution of the estimation problem becomes difficult. Inverse problems are unstable in nature because the unknown solutions have to be determined from indirect observable data which contain measurement errors. The major difficulty in establishing any numerical algorithm for approximating the solution is the ill-posedness of the problem and the ill-conditioning of the resulting discretized matrix. For instance, uniqueness and conditional stability results can be found in [2,3]. A number of techniques have been proposed for solving the inverse source problem, including the boundary element method (BEM) [4], iterative regularization methods [5–7] and mollification methods [8,9]. Besides, a sequential method [10] and linear least-squares error method [11] have also been used in solving the inverse source problem. In all of these methods, the partial differential equation must be discretized. The traditional mesh-dependent finite difference method (FDM) and finite element method (FEM) require a mesh on the domain to support the solution process, and hence tedious computational time. The BEM reduces the dimensionality of the problem by one, thus reduces the computational time. However, the main drawback

* Corresponding author.
E-mail addresses: yanliang06@lzu.cn (L. Yan), fuchuli@lzu.edu.cn (C.-L. Fu).

0021-9991/$ - see front matter © 2008 Elsevier Inc. All rights reserved.
doi:10.1016/j.jcp.2008.09.001

of the BEM is the evaluation of the singular integrals at the boundaries, which requires a great amount of computational effort.

In recent years, meshless methods have attracted great attention in the scientific and engineering community. Meshless methods emerge as a competitive alternative to mesh-dependent methods, including the radial basis functions (RBF) method [12,13], the method of fundamental solutions (MFS) [14,15] and the boundary knot method (BKM) [16,17]. These meshless methods require neither domain discretization as in the FEM and FDM, nor boundary discretization as in the BEM, thus they improve the computational efficiency and can be easily extended to solve high-order and high-dimensional differential equations. The MFS has been extensively applied to solve some engineering problems. However, the requirement of an arbitrary fictitious boundary outside the physical domain to avoid the singularity of the fundamental solution hinders its practical applicability. Some improved methods were introduced very recently. A number of authors used a non-singular solution instead of singular fundamental solution in the MFS, e.g. [16–19]. These methods dealt successfully with many kinds of problems and eliminated the well-known drawback of ambiguous off-set boundary. Another improved method is called the hybrid boundary node method [20,21], which combines the moving least squares interpolation scheme with the hybrid displacement variational formulation. Recently, Young et al. [22] developed a modified MFS, namely the regularized meshless method, to overcome the drawback of MFS for solving the Laplace equation.

In this paper, we extend the MFS to solve a spacewise-dependent inverse heat source problem under arbitrary geometry. More recently, Jin and Marin [23] employed the MFS to recover the heat source in steady-state heat conduction problems. In this reference the problem is reformulated by a fourth-order PDE using the a priori information that the source is harmonic or satisfies a Helmholtz equation. Yan et al. [24] also applied the MFS to identify a time-dependent heat source. Nevertheless, publications have not been found so far to use this method for solving the inverse problem of determining the heat source which is taken to be space-dependent only in the parabolic heat equation.

In this paper, we successfully changed the problem with only one unknown function and then applied the MFS technique on the resulted equation. Simultaneously, we introduce a time parameter T to avoid the singularities. The numerical results indicate that the accuracy of numerical solutions is relatively independent of this parameter. It should be noted that the MFS in conjunction with regularization methods has successfully been applied to inverse problems, such as inverse heat conduction problems [25,26] and the Cauchy problem for various partial differential equations [27–32].

The MFS discretized system of equations is ill-conditioned and hence it is solved by employing the Tikhonov regularization method, while the choice of the regularization parameter is based on the generalized cross-validation (GCV) criterion [38,42]. Several numerical examples for the inverse source problem are presented to demonstrate the efficacy of the proposed method.

2. Mathematical formulation of the problem

We consider a bounded domain $\Omega \subset R^d, d \geqslant 1$. Consider the following heat Eq. (1.1) in which the source $f(\mathbf{x}, t; u) = f(\mathbf{x})$ depends on space only and satisfies:

$$u_t = \Delta u + f(\mathbf{x}), \quad \mathbf{x} \in \Omega, t \in (0, t_{\max}], \tag{2.1}$$

with the initial condition

$$u(\mathbf{x}, 0) = 0, \quad \mathbf{x} \in \bar{\Omega}, \tag{2.2}$$

and the boundary condition

$$u(\mathbf{x}, t) = h(\mathbf{x}, t), \quad \mathbf{x} \in \partial\Omega, \quad t \in (0, t_{\max}], \tag{2.3}$$

where $h(\mathbf{x}, 0) = 0$ for $\mathbf{x} \in \partial\Omega$ in order to ensure the compatibility of the boundary condition (2.3) with the homogeneous initial condition (2.2). In this paper, we consider only the case that the initial condition is homogenous, however, using linearity one can also consider the case of a non-homogenous initial condition. Assume that the source function $f(\mathbf{x})$ is unknown, and the problem is mathematically underdetermined, such that additional data must be supplied to guarantee the uniqueness of the solution. In this paper, the additional data can be measured at a given time $t_0 \in (0, t_{\max}]$ in the domain Ω (e.g. [4]),

$$u(\mathbf{x}, t_0) = g(\mathbf{x}), \quad \mathbf{x} \in \Omega, \tag{2.4}$$

where $h(\mathbf{x}, t_0) = g(\mathbf{x})$ for $\mathbf{x} \in \partial\Omega$.

The inverse heat source problem is now formulated as follows: Reconstruct the temperature u and the heat source function $f(\mathbf{x})$ satisfying (2.1)–(2.4).

Remark. Under suitable conditions (see [5,6]), the inverse problem (2.1)–(2.4) has a unique solution.

Let us define the following transformation

$$v(\mathbf{x}, t) = u(\mathbf{x}, t) + r(\mathbf{x}), \tag{2.5}$$

$$\Delta r(\mathbf{x}) = f(\mathbf{x}). \tag{2.6}$$

It should be noted that in the transformation (2.6) the function $r(\mathbf{x})$ is not uniquely determined. In order to guarantee the uniqueness, we can assume that $r(\mathbf{x}) = 0$ for $\mathbf{x} \in \partial\Omega$. Although other formulations may be possible, in this study we investigate only the aforementioned formulation.

Using the above transformation, the problem (2.1)–(2.4) is transformed into the following problem:

$$v_t = \Delta v, \quad \mathbf{x} \in \Omega, \quad t \in (0, t_{\max}], \tag{2.7}$$

$$v(\mathbf{x}, 0) = r(\mathbf{x}), \quad \mathbf{x} \in \bar{\Omega}, \tag{2.8}$$

$$v(\mathbf{x}, t) = h(\mathbf{x}, t), \quad \mathbf{x} \in \partial\Omega, \quad t \in (0, t_{\max}] \tag{2.9}$$

$$v(\mathbf{x}, t_0) = g(\mathbf{x}) + r(\mathbf{x}), \quad \mathbf{x} \in \Omega. \tag{2.10}$$

It clearly follows by substituting (2.8) into (2.10) that v satisfies the following problem:

$$v_t - \Delta v = 0, \quad \mathbf{x} \in \Omega, \quad t \in (0, t_{\max}], \tag{2.11}$$

$$v(\mathbf{x}, t) = h(\mathbf{x}, t), \quad \mathbf{x} \in \partial\Omega, \quad t \in (0, t_{\max}] \tag{2.12}$$

$$v(\mathbf{x}, t_0) - v(\mathbf{x}, 0) = g(\mathbf{x}), \quad \mathbf{x} \in \Omega. \tag{2.13}$$

Once v is found, the unknown heat source can be calculated through the transformation (2.6) via numerical differentiation, i.e.

$$f(\mathbf{x}) = \Delta r(\mathbf{x}) = \Delta v(\mathbf{x}, 0). \tag{2.14}$$

This implies that the inverse spacewise-dependent heat source problem is mildly ill-posed. The instability of the solution to problem (2.11)–(2.14) can be shown by considering the following example in 1D case:

Let $\Omega = (0, \pi)$ and $t_0 = t_{\max} = 1$.

The solution of the problem (2.11)–(2.14) when

$$h = 0, \quad g = \frac{1 - e^{-n^2}}{n^{2-\epsilon}} \sin nx, \quad \epsilon \in (0, 1),$$

is given by

$$v(x, t) = -\frac{e^{-n^2 t}}{n^{2-\epsilon}} \sin nx.$$

Therefore, we have

$$\sup_{\bar{\Omega}}\{|h| + |g|\} = \mathcal{O}\left(\frac{1}{n^{2-\epsilon}}\right) \to 0, \quad n \to \infty,$$

but

$$\sup_{\Omega}\{|f(x)|\} = \sup_{\Omega}\{|v_{xx}(x, 0)|\} = n^{\epsilon} \to \infty, \quad n \to \infty.$$

This indicates that although the data $(|h| + |g|)$ tends to zero, the solution f is unbounded. In other words, the inverse spacewise-dependent heat source problem is ill-posed. It is in general very difficult to obtain a stable numerical solution to the problem (2.11)–(2.14) due to the ill-posedness of numerical differentiation. In the last decades, some computational methods have been suggested for numerical differentiation, see e.g. [33] and the extensive references therein.

Suppose that the given noisy data $\tilde{g}$ representing the measurement of the exact g satisfies

$$\|\tilde{g} - g\|_{L^2(\Omega)} \leqslant \delta, \tag{2.15}$$

where δ is a positive constant representing the noise level of the input data. We aim at finding an approximate function $v^*(\mathbf{x}, t)$ of $v(\mathbf{x}, t)$ such that $\|\Delta v^*(\mathbf{x}, 0) - f(\mathbf{x})\|$ converges to zero, as δ tends to zero. In the following section, we develop a numerical method based on the MFS with regularization to solve the problem (2.11)–(2.15).

3. Method of fundamental solutions and regularization

In this section, we describe the numerical scheme for the inverse spacewise-dependent heat source problem, namely the MFS in conjunction with the Tikhonov regularization (TR). Rules for choosing an appropriate regularization parameter are also detailed. The MFS is an inherently meshless boundary-type technique for the solution of partial differential equations. The basic idea of the method is to approximate the solution of the governing partial differential equation by a linear combination of fundamental solutions with singularities, also known as source points, located on a fictitious boundary outsider the solution domain. For denseness results of the method for the forward time-dependent heat equation, we refer the reader to [34,35].

The fundamental solution of Eq. (2.11) is given by

$$F(\mathbf{x},t)=\frac{1}{(4\pi t)^{\frac{d}{2}}}e^{-\frac{|\mathbf{x}|^2}{4t}}H(t), \tag{3.1}$$

where $H(t)$ is the Heaviside function. Assume that $T>t_{\max}$ is a constant. Then the following time shift function

$$\phi(\mathbf{x},t)=F(\mathbf{x},t+T), \tag{3.2}$$

is a non-singular solution of Eq. (2.11) in the domain $\bar{\Omega}\times[0,t_{\max}]$.

Let $\{(\mathbf{x}_j,t_j)\}_{j=1}^{m}$ denote the measurement points in the region $\Omega\times\{t_0\}$. The boundary collocation points are chosen as $\{(\mathbf{x}_j,t_j)\}_{j=m+1}^{m+n}$ on the surface $\partial\Omega\times(0,t_{\max}]$. Following the idea of the MFS, we assume that an approximation to the solution of the problem (2.11)–(2.14) can be expressed by the following linear combination:

$$v^*(\mathbf{x},t)=\sum_{j=1}^{m+n}\lambda_j\phi(\mathbf{x}-\mathbf{x}_j,t-t_j), \tag{3.3}$$

where the basis function $\phi(\mathbf{x},t)$ is given by Eq. (3.2) and λ_j are unknown coefficients to be determined. From (3.2) to (3.3), we can see that the source points are placed at the same spatial positions but at different time levels. It is well-known that the accuracy of the MFS depends on the choice of the parameter T. However, treating the additional parameter T to be optimized, would complicate even further the difficult inverse and ill-posed problem under investigation and therefore, this analysis is deferred to a future work. For different ideas of choosing the source points in MFS for the time-dependent heat equation, see [24,25,36,37].

For the choice (3.2) of basis function ϕ, the approximated solution v^* satisfies the heat Eq. (2.11) automatically. Using the conditions (2.12) and (2.13), we then obtain the following system of linear equations for the unknown coefficients λ_j:

$$\mathbf{A}\lambda=\mathbf{b}, \tag{3.4}$$

where

$$\mathbf{A}=\begin{pmatrix}\phi(\mathbf{x}_i-\mathbf{x}_j,t_0-t_j)-\phi(\mathbf{x}_i-\mathbf{x}_j,0-t_j)\\ \phi(\mathbf{x}_k-\mathbf{x}_j,t_k-t_j)\end{pmatrix}, \tag{3.5}$$

and

$$\mathbf{b}=\begin{pmatrix}\tilde{g}_i\\ h(\mathbf{x}_k,t_k)\end{pmatrix}, \tag{3.6}$$

where $i=1,2,\ldots,m;\ k=m+1,\ldots,m+n;\ j=1,2,\ldots,m+n$. The system of linear algebraic Eq. (3.4) cannot be solved by direct methods, such as the least-squares (LS) method, since such an approach would produce a highly unstable solution due to the large value of the condition number of the matrix $\mathbf{A}$ which increases dramatically as the number of collocation points increases [14]. Several regularization procedures have been developed to solve such ill-conditioned system, see for example Hansen [38]. One of the most used regularization technique is the Tikhonov regularization (TR) method [40]. The Tikhonov regularized solution λ_α for the system of Eq. (3.4) is defined as the solution of the following minimization problem:

$$\min_{\lambda}\{||\mathbf{A}\lambda-\mathbf{b}||^2+\alpha||\lambda||^2\}, \tag{3.7}$$

where $\|\cdot\|$ denotes the Euclidean norm and $\alpha>0$ is called the regularization parameter. The choice of a suitable value of the regularization parameter α is crucial for the accuracy of the final numerical solution and is still under intensive research [41]. One parameter choice criterion extensively studied is the discrepancy principle [39], however, it requires a reliable estimation of the amount of noise δ in the data, see Eq. (2.15). Heuristical approaches are preferable in the case when no a priori information about the noise is available. For the TR method, several heuristical approaches have been proposed, including the L-curve criterion [38], cross-validation (CV), and generalized cross validation (GCV) [42]. In this paper, we use the GCV to choose the regularization parameter. In GCV the regularization parameter α is chosen to minimize the GCV function

$$G(\alpha)=\frac{||\mathbf{A}\lambda_\alpha-\mathbf{b}||^2}{(\mathrm{trace}(I_{n+m}-\mathbf{A}\mathbf{A}^I))^2},\quad \alpha>0, \tag{3.8}$$

where $\mathbf{A}^I=(\mathbf{A}^{tr}\mathbf{A}+\alpha I_{n+m})^{-1}\mathbf{A}^{tr}$.

Denote the regularized solution by λ^{α^*}, then the approximate solution for the problem (2.11)–(2.14) can be written as

$$v^*_\alpha(\mathbf{x},t)=\sum_{j=1}^{m+n}\lambda_j^{\alpha^*}\phi(\mathbf{x}-\mathbf{x}_j,t-t_j), \tag{3.9}$$

$$r^*(\mathbf{x}) = \sum_{j=1}^{m+n} \lambda_j^{\alpha^*} \phi(\mathbf{x} - \mathbf{x}_j, 0 - t_j). \tag{3.10}$$

The solution of problem (2.1)–(2.4) is then given by

$$u^*(\mathbf{x}, t) = v_\alpha^*(\mathbf{x}, t) - r^*(\mathbf{x}), \tag{3.11}$$

and

$$f^*(\mathbf{x}) = \Delta r^*(\mathbf{x}) = \sum_{j=1}^{m+n} \lambda_j^{\alpha^*} \Delta\phi(\mathbf{x} - \mathbf{x}_j, 0 - t_j). \tag{3.12}$$

4. Numerical experiments

For simplicity, we set $t_{\max} = 1$ in all the following examples. We use the function *rand* given in Matlab to generate the noisy data $\tilde{g}_i = g_i + 2\delta(rand(i) - 0.5)$, where g_i is the exact data and $rand(i)$ denotes a random number from the uniform distribution of interval $(0, 1)$. The magnitude δ indicates the noise level of measurement data.

Although neither convergence nor estimate proofs are as yet available for the MFS, the numerical results presented in this section for the inverse heat source problem indicate that the proposed method is feasible and efficient. In order to present the performance of the MFS in conjunction with the TR method, we first define the root mean square error (RMS) and the relative root mean square error (RES) as

$$\mathrm{RMS}(f) = \sqrt{\frac{1}{N_t} \sum_{i=1}^{N_t} (f(\widetilde{\mathbf{x}}_i) - f^*(\widetilde{\mathbf{x}}_i))^2}, \tag{4.1}$$

$$\mathrm{RES}(f) = \frac{\sqrt{\sum_{i=1}^{N_t} (f(\widetilde{\mathbf{x}}_i) - f^*(\widetilde{\mathbf{x}}_i))^2}}{\sqrt{\sum_{i=1}^{N_t} (f(\widetilde{\mathbf{x}}_i))^2}}, \tag{4.2}$$

where N_t is the total number of testing points in the domain $\bar{\Omega}$, $f(\widetilde{\mathbf{x}}_i)$, $f^*(\widetilde{\mathbf{x}}_i)$ are, respectively, the exact and approximated value at these points.The RMS and RES for the heat temperature RES(u) and RES(u) are also similarly defined.

4.1. One-dimensional examples

Example 1. The exact solution of problem (2.1)–(2.4) with $h = 0$ and $g(x) = (1 - \mathrm{e}^{-\pi^2}) \sin \pi x$ is given by

$$u(x, t) = (1 - \mathrm{e}^{-\pi^2 t}) \sin \pi x, \quad (x, t) \in [0, 1] \times [0, 1], \tag{4.3}$$

$$f(x) = \pi^2 \sin \pi x, \quad x \in [0, 1]. \tag{4.4}$$

Example 2. We consider an example where there is no analytical solution available. To obtain the data (2.4), we first solve the following direct problem by using the standard Crank–Nicholson (CN) difference scheme:

$$\begin{aligned} &u_t = u_{xx} + f(x), \quad (x, t) \in (0, 1) \times (0, 1], \\ &u(0, t) = u(1, t) = 0, \quad t \in (0, 1], \\ &u(x, 0) = 0, \quad x \in [0, 1], \end{aligned}$$

where

$$f(x) = \begin{cases} 0, & 0 \leqslant x \leqslant 0.25, \\ 4(x - 0.25), & 0.25 < x \leqslant 0.5, \\ -4(x - 0.75), & 0.5 < x \leqslant 0.75, \\ 0, & 0.75 < x \leqslant 1. \end{cases} \tag{4.5}$$

Unless otherwise specified, the parameter T is taken to be 1.5 and t_0 is taken to be 1. We also choose typically $m = 11, n = 22, N_t = 21$. The inverse heat source problems investigated in this study have been solved using a uniform distribution of both the collocation points and measurement points.

We consider Example 1 with noise of level $\delta = 0.01$ added into the data (2.4). Fig. 1(a) presents the exact and numerical solutions for the heat source $f(x)$, obtained using the LS method. It can be seen from this figure that the LS method gives an unstable solution to the problem. The large oscillations in the solution are due to the contributions from the small singular

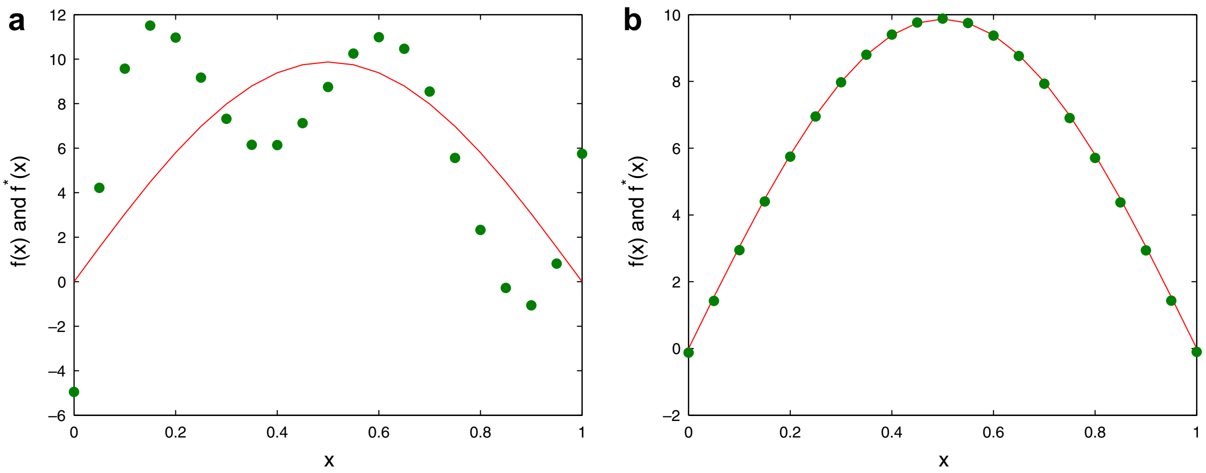

Fig. 1. The numerical solution for the heat source $f(x)$ and its approximation $f^*(x)$ obtained using 1% noise added into the data. (a) LS method; (b) TR method, for Example 1.

values and the presence of noise in the data. From Fig. 2(a) it can be seen that there are numerous small singular values in the singular value spectrum of the matrix **A**. The condition number of the matrix **A** for this example is approximately 4.18×10^{17}, which is enormous compared with the size of the interpolation matrix. Here the condition number is defined as the ratio of the largest singular value to the smallest singular value.

The numerical results obtained using the TR method and the corresponding GCV function (3.8) are presented in Figs. 1 and 2(b), respectively. Compared with the results by the LS method, the results by TR method are far more accurate. Therefore, the TR method is indispensable to obtained accurate and stable results for ill-posed problems with noisy data. The numerical results with various noise levels for Example 1 are shown in Fig. 3. From this figure it can be seen that the results are quite satisfactory, even with the noise level up to $\delta = 0.05$. Furthermore, by comparing Figs. 2(b) and 3, we can see that the choice of the regularization parameter α^* according to the GCV is fully justified.

In order to investigate the influence of the parameter T on the accuracy and stability of the numerical solutions for the temperature and the heat source, we consider Example 1 with noise data ($\delta = 0.01$). In Fig. 4 we present the errors RMS and RES for Example 1 as functions of the parameter T. It can be seen from this figure that the accuracy of the numerical results is relatively independent of the parameter T if $T < 4$. The insensitivity of the solutions to T over fairly large ranges of the parameters is a favorable feature of MFS because there is no need to search for optimal values of parameters.

Next, we analyze the accuracy of the numerical method proposed with respect to the parameter t_0. To do so, we set $T = 1.5$ for the inverse problem given by Example 1. Fig. 5 illustrate the errors RMS and RES as functions of t_0. From this figure it can be seen that both errors decrease as the parameter t_0 increases and, in addition, these errors do not decrease for $t_0 \geqslant 0.6$.

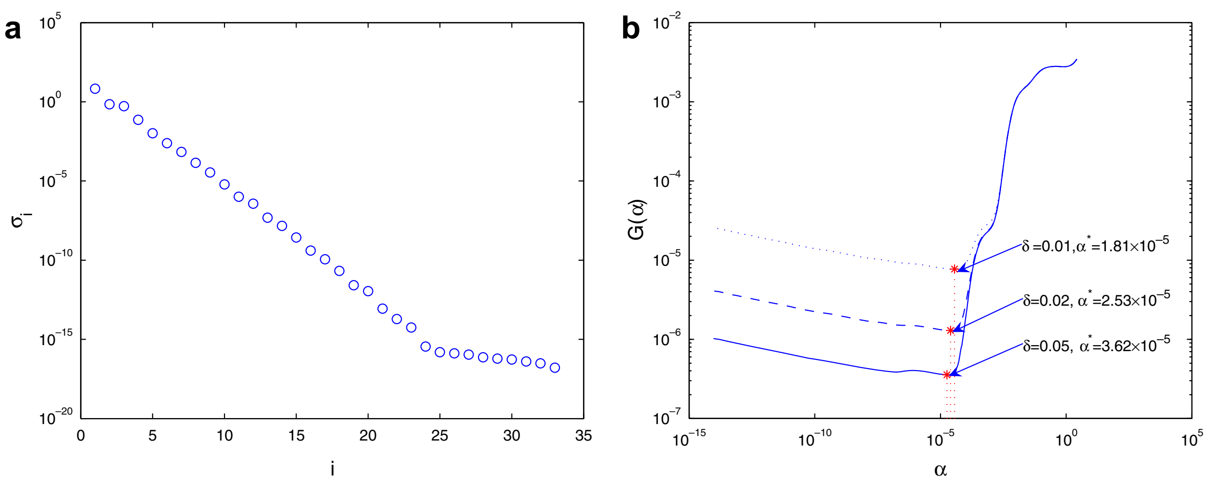

Fig. 2. (a) The singular value spectrum; and (b) the GCV plot, for Example 1.

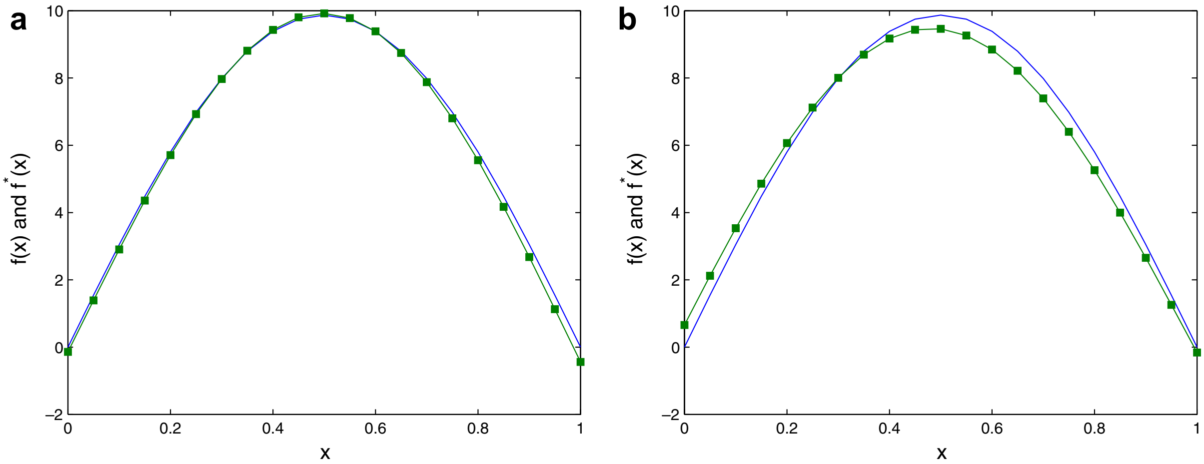

Fig. 3. The numerical results for Example 1 with (a) 2% and (b) 5% noise in the data.

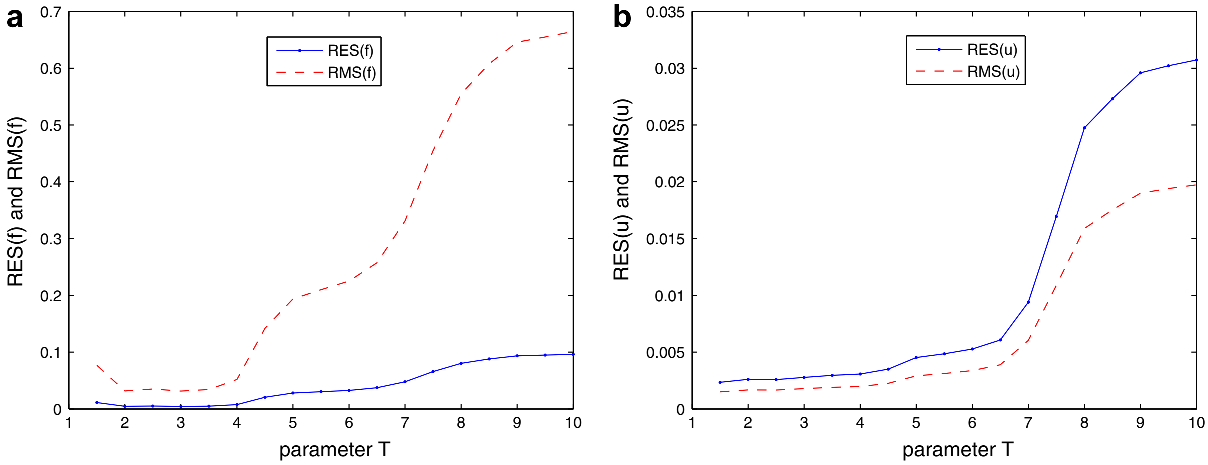

Fig. 4. The accuracy of the numerical solutions for Example 1 with $\delta = 1\%$ with respect to the parameter T.

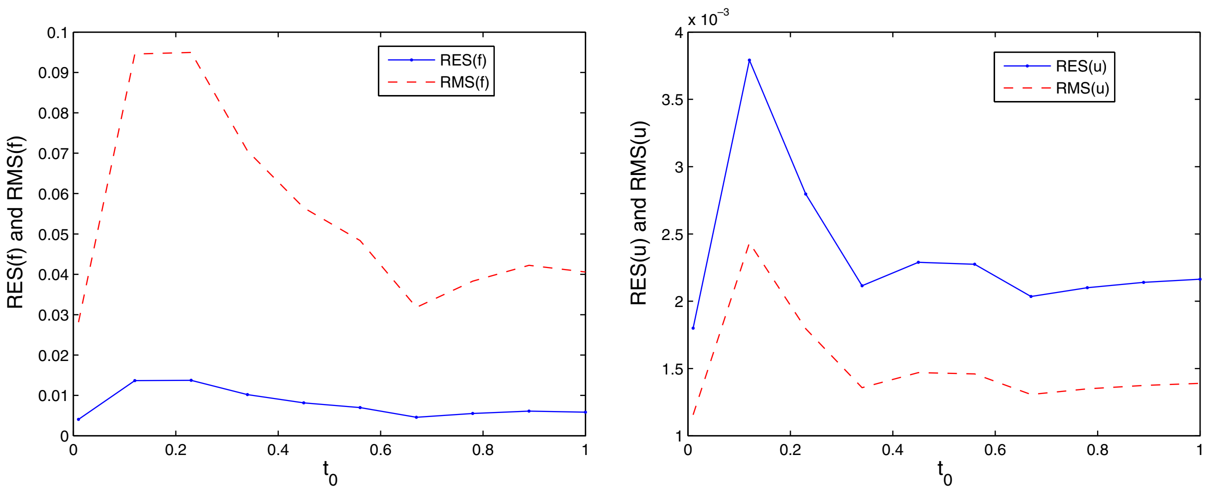

Fig. 5. The accuracy of the numerical solutions for Example 1 with $\delta = 1\%$ with respect to the parameter t_0.

The method works equally well for problems for which there is no analytical solution available. To illustrate this, the numerical results obtained for Example 2 using various amounts of noise added into the data are presented in Fig. 6. From this figure it can be seen that the numerical results are less accurate than those of Example 1. It is not difficult to see that the recovered data where $x \leqslant 0.2$ and $x \geqslant 0.8$ are not accurate indicating that the method employed fails to recover non-smooth sources. However, taking into consideration the ill-posedness of the problems investigated, the results presented here are quite satisfactory.

4.2. Two-dimensional examples

For two-dimensional problems, the solution domains under consideration are the following three cases:

Case 1.

$$\Omega = \{(x_1, x_2) | 0 < x_1 < 1, 0 < x_2 < 1\}. \tag{4.6}$$

Case 2.

$$\Omega = \{(x_1, x_2) | x_1^2 + x_2^2 < 1\}. \tag{4.7}$$

Case 3. (Complex geometry): The configuration of the complicated case is schematically shown in Fig. 7(c). This case is to verify the efficiency and effectiveness of the proposed scheme when dealing with problems related to an arbitrary geometry.

For the convenience of comparison and illustration of the accuracy of the method, we consider inverse problems with analytical solutions as listed in Table 1. The boundary data $h(x_1, x_2, t)$ is computed from the known solutions u. The values of the temperature g_i at measurement points are also obtained from the given solutions. Locations of the internal measurements and boundary collocation points over the domain $\bar{\Omega}$ for the test cases are shown in Fig. 7. The location of source points coincides with that of collocation points. Unless otherwise specified, $T = 1.9$, $t_0 = 1$ in all cases, and the other parameters did not significantly improve the accuracy of the numerical results. The total numbers of various boundary collocation, measurement and testing points are given in Table 2.

The proposed numerical scheme is accurate for problems with exact data. For instance, the error distribution for the numerical heat source obtained using exact data for Example 3 are displayed in Fig. 8. The maximum error is less than 3.9×10^{-3} for the LS method and is less than 1.17×10^{-5} for TR method, respectively. Thus TR method seems to be capable of improving the accuracy of the results significantly for exact data.

The error distribution for the numerical heat sources obtained for, using various amounts of noise added into the data, are presented in Fig. 9. It can be seen from these figures that the numerical results retrieved for the heat source represent good approximations for their analytical values. Furthermore, the numerical heat sources converge towards their corresponding exact solutions as the amount of noise decreases. Similar results have been obtained for Example 4 and these are illustrated in Fig. 10. Hence the MFS, in conjunction with the TR method, provides stable numerical solutions to the 2-D inverse source problem with smooth geometry.

The values for the accuracy errors RMS(f) and RES(f), the condition number cond($\mathbf{A}$) of the interpolation matrix $\mathbf{A}$ and the regularization parameter α^* as given by the GCV, are presented in Table 3, obtained with the noise level $\delta = 0.02$ added into the data for all the 2-D examples investigated. It can be seen from this table that the error in the numerical solution is maintained at a small and comparable level with that in the data.

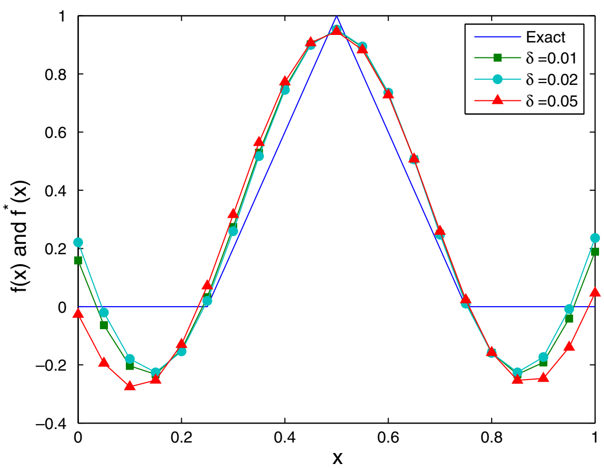

Fig. 6. The numerical results obtained using the TR method for various amounts of noise added into the data for Example 2.

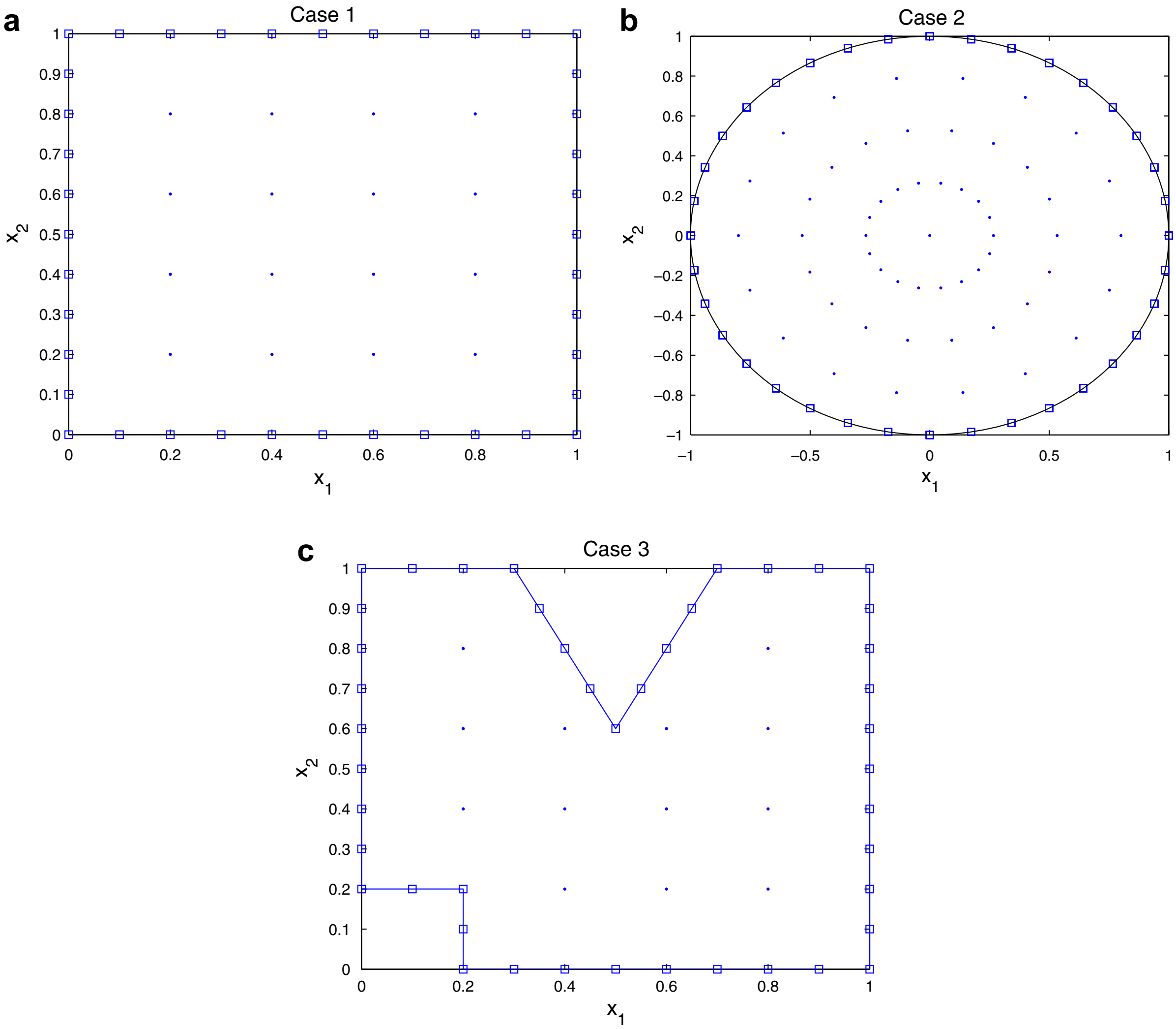

Fig. 7. Distribution of measurement and collocation points. Here, square represents boundary collocation points on $\partial\Omega$, dot represents measurement points in Ω at t_0.

Table 1
Test cases for inverse source problems

Example	$u(\mathbf{x},t)$	$f(\mathbf{x})$	Domain
3	$(1-e^{-4t})(\cos(2x_1)+\cos(2x_2))$	$4(\cos(2x_1)+\cos(2x_2))$	Case 1
4	$\frac{t}{2}(x_1+x_2)$	$\frac{1}{2}(x_1+x_2)$	Case 2
5	$\frac{t}{2}(x_1+x_2)$	$\frac{1}{2}(x_1+x_2)$	Case 3

Table 2
The setup for the solution of the test cases

	m	n	N_t
Case 1	16	200	121
Case 2	55	180	145
Case 3	13	220	121

So far, we have investigated the scheme only for inverse problems in a simple geometry. In fact, the proposed method works equally well for inverse problems in a complicated geometry. To illustrate this, we consider Example 5. The numerical results for Example 5 are presented in Fig. 11. With up to 2% noise in the data, the numerical results are found to be in good

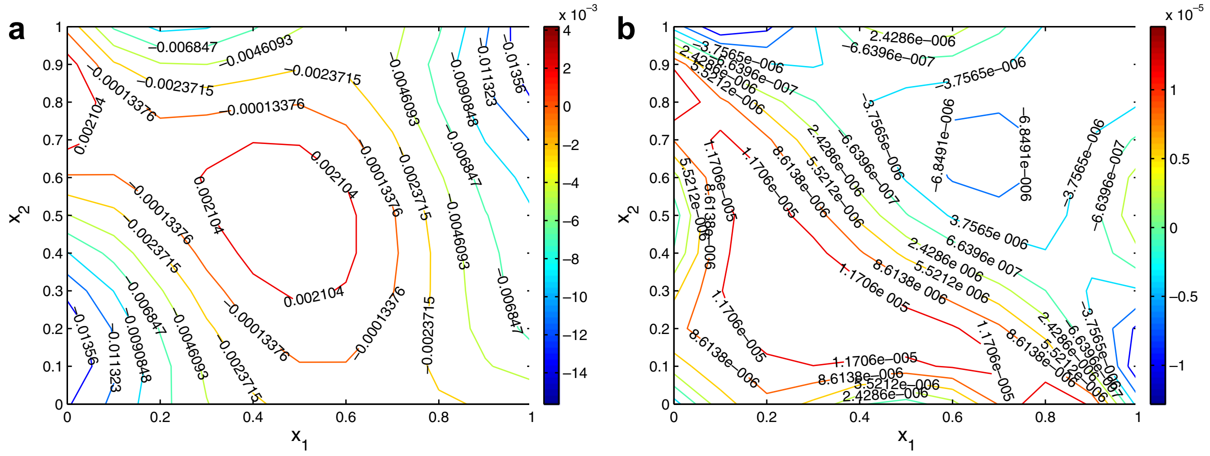

Fig. 8. The error distribution for $f(\mathbf{x})$ obtained using exact data, (a) Least-squares method; and (b) the TR method, for Example 3.

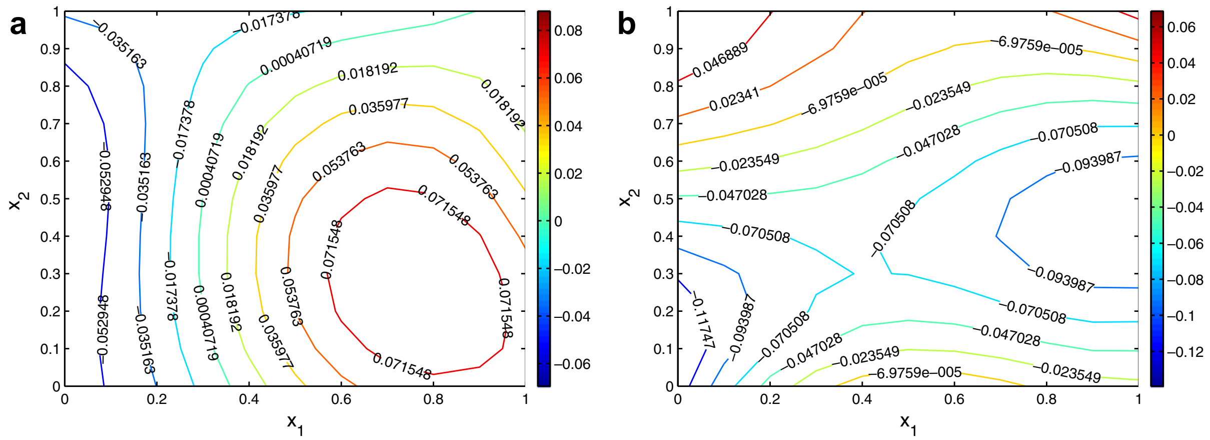

Fig. 9. The error distribution for $f(\mathbf{x})$ obtained using the TR method for various amounts of noise added into the data, namely: (a) 1%; and (b) 2%, for Example 3.

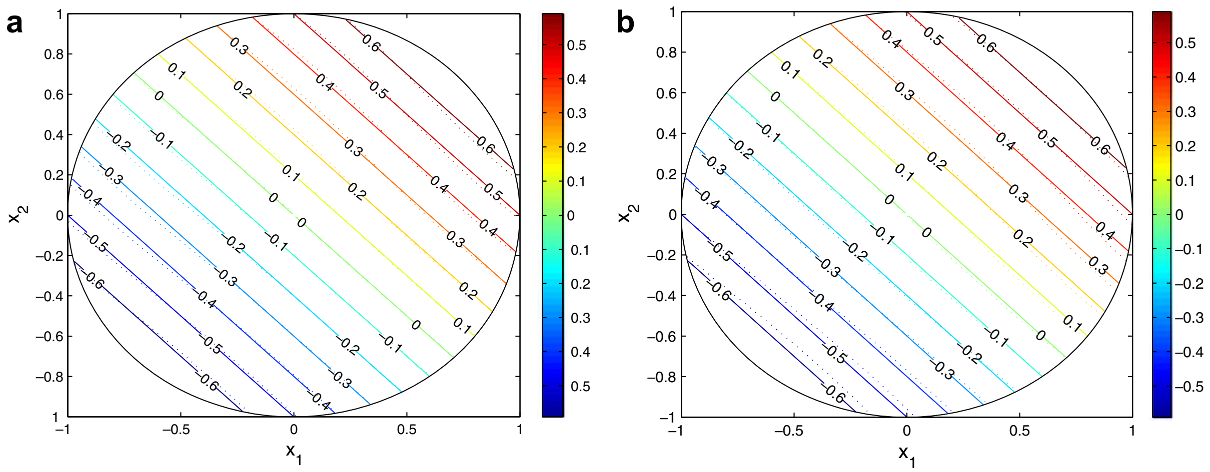

Fig. 10. The exact (–) and numerical (···) heat source obtained using the TR method for various amounts of noise added into the data, namely: (a) 1%; and (b) 2%, for Example 4.

Table 3
The accuracy of the numerical results for the test cases with $\delta = 0.02$

Example	Cond(**A**)	α^*	RMS(f)	RES(f)
3	1.49×10^{19}	3.98×10^{-7}	0.0144	0.0639
4	1.79×10^{19}	1.16×10^{-5}	0.0213	0.0729
5	1.01×10^{19}	5.38×10^{-5}	0.0227	0.0428

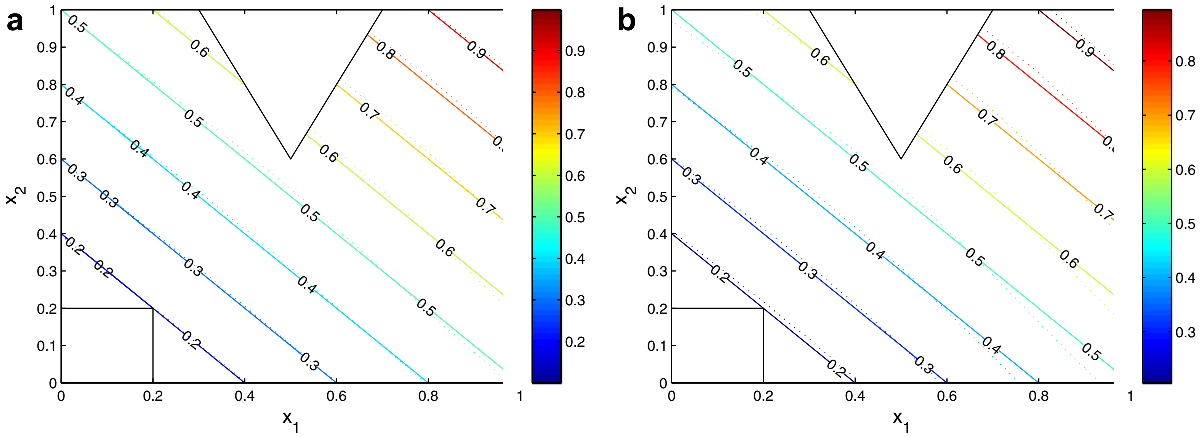

Fig. 11. The exact (–) and numerical (···) heat source obtained using the TR method for various amounts of noise added into the data, namely: (a) 1%; and (b) 2%, for Example 5.

agreement with the exact solution. The accuracy of the numerical results achieved is comparable with that for problems with smooth geometry, as indicated in Table 3. These results show clearly that the present scheme works equally well for problems with complicated geometry.

4.3. Three-dimensional example

Three-dimensional heat problems are usually not easy to deal with partly due to the expensive effort in the mesh generation for mesh-dependent techniques and, more importantly, due to the exponential increasing size of the resulting analogous discrete equations. This fact is the so-called curse of dimensionality. The following example is intended to verify numerically the accuracy and efficiency of the present MFS + TR solution for a 3-D problem.

Example 6. Let

$$\Omega = \{(x_1, x_2, x_3) | 0 < x_i < 1, i = 1, 2, 3\}. \tag{4.8}$$

The location of measurement points and collocation points in the domain Ω are shown in Fig. 12. In this computation, we take $m = 64, n = 760, N_t = 21^3$. The exact solution for Example 6 is given by

$$u(x_1, x_2, x_3, t) = (1 - e^{-4t})(\cos(2x_1) + \cos(2x_2) + \cos(2x_3)), \tag{4.9}$$

$$f(x_1, x_2, x_3) = 4(\cos(2x_1) + \cos(2x_2) + \cos(2x_3)). \tag{4.10}$$

In this computation, the value of the parameter T is 3.5. The exact and numerical results for the heat source $f(\mathbf{x})$ on the surfaces $\{(x_1, x_2, 0) \mid 0 < x_1, x_2 < 1\}$ and $\{(x_1, x_2, 0.5) \mid 0 < x_1, x_2 < 1\}$ obtained with $\delta = 2\%$ noise added into the data, for the three-dimensional inverse spacewise-dependent heat source problem as given by Example 6, are shown in Fig. 13(a) and (b), respectively, while their corresponding error distributions are illustrated in Fig. 13(c) and (d), respectively. It can be seen from these figures that the numerical results are in good agreement with their corresponding exact solutions. The numerical results for relative noise level $\delta = [10^{-5} - 10^{0}, 2, 5, 10]\%$ are reported in Fig. 14. It can be seen from this figure that the MFS approximation provides very accurate numerical results. Furthermore, both RES(f) and RMS(f) decrease as the level of noise δ added into the data decreases and RES(f) < RMS(f) for a fixed δ. From Figs. 13 and 14 we can conclude that the MFS + TR works as well for this 3-D problem as in the previous 2-D cases.

Overall, we can conclude that the proposed method, i.e. the MFS in conjunction with the TR method, is an accurate and reliable numerical tool for the solution of the inverse heat source problem.

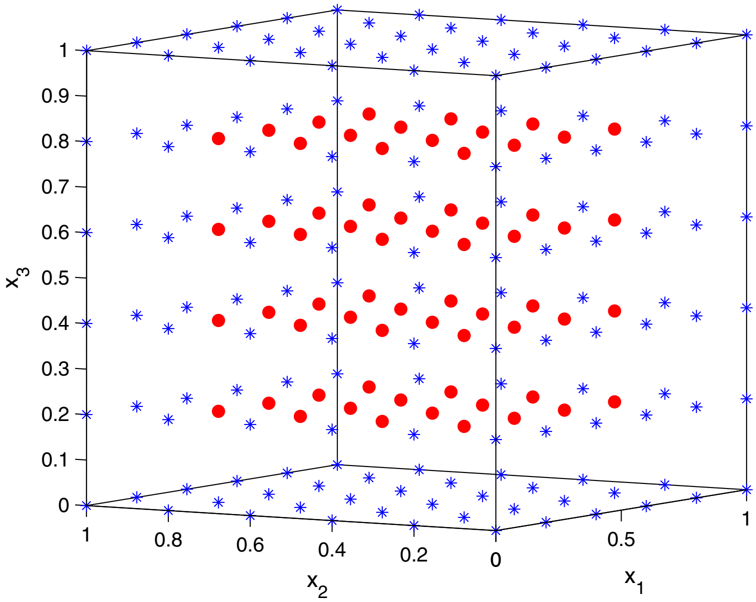

Fig. 12. Locations of measurement and collection points. Star represents bountry collection points, dot represents measurement points in Ω at t_0.

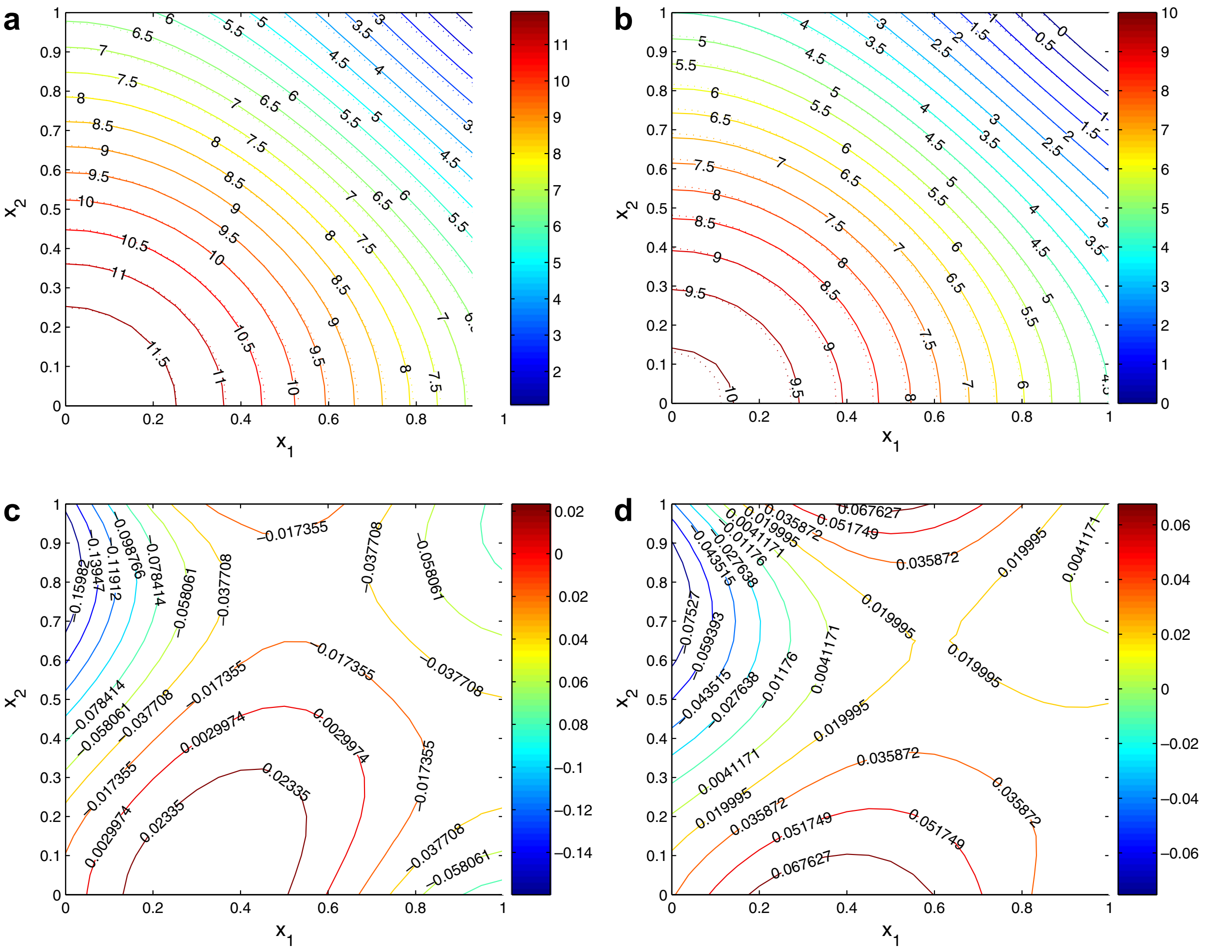

Fig. 13. The exact (–) and numerical (⋯) heat source (a) $f(x_1, x_2, 0)$, and (b) $f(x_1, x_2, 0.5)$, and the error distribution corresponding to (c) $f(x_1, x_2, 0)$, and (d) $f(x_1, x_2, 0.5)$, obtained using the TR method and $\delta = 2\%$ noise added into the data, for Example 6.

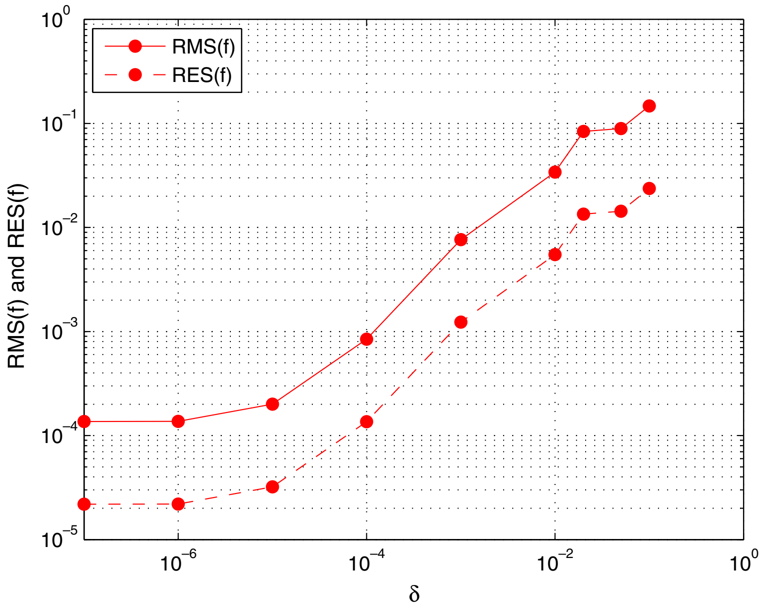

Fig. 14. The numerical results obtained using various amounts of noise added into the data for Example 6.

5. Conclusion

In this paper, we have implemented the MFS to solve a spacewise dependent heat source problem for arbitrary domains based on the Tikhonov regularization method with the GCV criterion. We successfully changed the equation with only one unknown function and then applied the MFS technique to the resulted equation. The numerical results show that the MFS is an accurate and reliable numerical technique for the solution of the inverse heat source problem and the accuracy of numerical solutions is relatively independent of the parameter T. Moreover, the proposed method is readily extendable to solve higher dimensional problems with complicated and irregular domains.

Acknowledgments

The authors gratefully thank Professor Lesnic Daniel for his kind provision of relevant literature and the referees for their valuable constructive comments which improve greatly the quality of the paper. The project is supported by the NNSF of China (Nos. 10671085 and 10571079).

References

[1] J. Hadamard, Lectures on the Cauchy Problem in Linear Partial Differential Equations, Oxford University Press, London, 1923.
[2] J.R. Cannon, E.S. Pérez, Uniqueness and stability of 3D heat sources, Inverse Probl. 7 (1991) 57–62.
[3] M. Choulli, M. Yamamoto, Conditional stability in determining a heat source, J. Inverse Ill-posed Probl. 12 (2004) 233–243.
[4] A. Farcas, D. Lesnic, The boundary-element method for the determination of a heat source dependent on one variable, J. Eng. Math. 54 (2006) 375–388.
[5] B.T. Johansson, D. Lesnic, Determination of a spacewise dependent heat source, J. Comput. Appl. Math. 209 (2007) 66–80.
[6] B.T. Johansson, D. Lesnic, A variational method for identifying a spacewise-dependent heat source, IMA J. Appl. Math. 72 (6) (2007) 748–760.
[7] B.T. Johansson, D. Lesnic, A procedure for determining a spacewise dependent heat source and the initial temperature, Appl. Anal. 87 (2008) 265–276.
[8] Zh. Yi, D.A. Murio, Source term identification in 1-D IHCP, Comput. Math. Appl. 47 (2004) 1921–1933.
[9] Zh. Yi, D.A. Murio, Source term identification in 2-D IHCP, Comput. Math. Appl. 47 (2004) 1517–1533.
[10] C.Y. Yang, A sequential method to estimate the strength of the heat source based on symbolic computation, Int. J. Heat Mass. Transfer 41 (14) (1998) 2245–2252.
[11] C.Y. Yang, Solving the two-dimensional inverse heat source problem through the linear least-squares error method, Int. J. Heat Mass Transfer 41 (2) (1998) 393–398.
[12] M.D.J. Powell, Radial basis functions for multivariable interpolation: a review, in: D.F. Griffiths, G.A. Watson (Eds.), Numerical Analysis, Longman Scientific and Technical, Harlow, 1987, pp. 223–241.
[13] Z. Wu, Hermite–Birkhoff interpolation for scattered data by radial basis function, Approxim. Theory Appl. 8 (2) (1992) 1–10.
[14] M.A. Golberg, C.S. Chen, The method of fundamental solutions for potential hemholtz and diffusion problems, in: Boundary Integral Methods: Numerical and Mathematical Aspects, Computational Mechanics Publication, Southampton, 1999, pp. 103–176.
[15] G. Fairweather, A. Karageorghis, The method of fundamental solutions for elliptic boundary value problems, Adv. Comput. Math. 9 (1–2) (1998) 69–95.
[16] W. Chen, Y.C. Hon, Numerical investigation on convergence of boundary knot method in the analysis of homogeneous Helmholtz, modified Helmholtz, and convection-diffusion problems, Comput. Methods Appl. Mech. Eng. 192 (2003) 1859–1875.
[17] W. Chen, M. Tanaka, A meshless, integration-free, and boundary-only RBF technique, Comput. Math. Appl. 43 (3–5) (2002) 379–391.
[18] J.T. Chen, I.L. Chen, K.H. Chen, Y.T. Lee, Y.T. Yeh, A meshless method for free vibration analysis of circular and rectangular clamped plates using radial basis function, Eng. Anal. Boundary Elements 28 (2004) 535–545.

[19] S.W. Kang, J.M. Lee, Y.J. Kang, Vibration analysis of arbitrary shape membranes using non-dimensional dynamic influence function, J. Sound Vib. 221 (1) (1999) 117–132.
[20] J.M. Zhang, M. Tanaka, T. Matsumoto, Meshless analysis of potential problems in three dimensions with the hybrid boundary node method, Int. J. Numer. Meth. Eng. 59 (2004) 1147–1160.
[21] J.M. Zhang, Z.H. Yao, H. Li, A hybrid boundary node method, Int. J. Numer. Meth. Eng. 53 (2002) 751–763.
[22] D.L. Young, K.H. Chen, C.W. Lee, Novel meshless method for solving the potential problems with arbitrary domain, J. Comput. Phys. 209 (2005) 290–321.
[23] B. Jin, L. Marin, The method of fundamental solutions for inverse source problems associated with the steady-state heat conduction, Int. J. Numer. Meth. Eng. 69 (2007) 1570–1589.
[24] L. Yan, C.L. Fu, F.L. Yang, The method of fundamental solutions for the inverse heat source problem, Eng. Anal. Boundary Elements 32 (2008) 216–222.
[25] Y.C. Hon, T. Wei, A fundamental solution method for inverse heat conduction problem, Eng. Anal. Boundary Elements 28 (2004) 489–495.
[26] Y.C. Hon, T. Wei, Numerical computation for multidimensional inverse heat conduction problem, CMES: Comput. Model. Eng. Sci. 7 (2005) 119–132.
[27] T. Wei, Y.C. Hon, L. Ling, Method of fundamental solutions with regularization techniques for Cauchy problems of elliptic operators, Eng. Anal. Boundary Elements 31 (2007) 373–385.
[28] L. Marin, D. Lesnic, The method of fundamental solutions for the Cauchy problem associated with two-dimensional Helmholtz-type equations, Comput. Struct. 83 (4–5) (2005) 267–278.
[29] L. Marin, D. Lesnic, The method of fundamental solutions for inverse boundary value problems associated with the two-dimensional biharmonic equation, Math. Comput. Model. 42 (2005) 261–278.
[30] L. Marin, D. Lesnic, The method of fundamental solutions for nonlinear functionally graded materials, Int. J. Solids Struct. 44 (2007) 6878–6890.
[31] N.S. Mera, D. Lesnic, A three-dimensional boundary determination problem in potential corrosion damage, Comput. Mech. 36 (2005) 129–138.
[32] B. Jin, Y. Zheng, A meshless method for some inverse problems associated with the Helmholtz equation, Comput. Meth. Appl. Mech. Eng. 195 (19–22) (2006) 2270–2288.
[33] T. Wei, Y.C. Hon, Numerical differentiation by radial basis functions approximation, Adv. Comput. Math. 27 (2007) 247–272.
[34] V.D. Kupradze, A method for the approximate solution of limiting problems in mathematical physics, USSR Comput. Maths. Math. Phys. 4 (1964) 199–205.
[35] B.T. Johansson, D. Lesnic, A method of fundamental solutions for transient heat conduction, Eng. Anal. Boundary Elements 32 (2008) 697–703.
[36] D.L. Young, C.C. Tsai, K. Murugesan, C.M. Fan, C.W. Chen, Time-dependent fundamental solutions for homogeneous diffusion problems, Eng. Anal. Boundary Elements 28 (2004) 1463–1473.
[37] S. Chantasiriwan, Methods of fundamental solutions for time-dependent heat conduction problems, Int. J. Numer. Meth. Eng. 66 (2006) 147–165.
[38] P.C. Hansen, Rank-Deficient and Discrete Ill-Posed Problems, SIAM, Philadelphia, 1998.
[39] V.A. Morozov, Methods for solving Incorrectly Posed Problems, Springer, New York, 1984.
[40] H.W. Engl, M. Hanke, A. Neubauer, Regularization of Inverse Problems, Mathematics, and its Applications, vol. 357, Kluwer Academic Publishers, Dordrecht, 1996.
[41] U. Tautenhahn, U. Hämarik, The use of monotonicity for choosing the regularization parameter in ill-posed problems, Inverse Probl. 15 (1999) 1487–1505.
[42] G. Golub, M. Heath, G. Wahba, Generalized cross-validation as a method for choosing a good ridge parameter, Technometrics 21 (2) (1979) 215–223.